Chemical Physics Letters 552 (2012) 114–121

Contents lists available at SciVerse ScienceDirect

Chemical Physics Letters

journal homepage: www.elsevier.com/locate/cplett

Dielectric spectroscopy and molecular dynamics of epoxy oligomers with covalently bonded nonlinear optical chromophores

N.A. Nikonorova [a,*], M.Yu. Balakina [b], O.D. Fominykh [b], M.S. Pudovkin [b], T.A. Vakhonina [b], R. Diaz-Calleja [c], A.V. Yakimansky [a]

[a] Institute of Macromolecular Compounds RAS, Bolshoi pr., 31, 199004 Saint-Petersburg, Russia
[b] A.E. Arbuzov Institute of Organic and Physical Chemistry KSC RAS, 420088 Kazan, Russia
[c] Polytechnic University of Valencia, Electrical Technology Institute, Camino de Vera s/n, 46022 Valencia, Spain

ARTICLE INFO

Article history:
Received 6 July 2012
In final form 24 September 2012
Available online 28 September 2012

ABSTRACT

Dielectric behavior of two epoxy-based oligomers with covalently attached 4-amino-4′-nitroazobenzene NLO chromophore fragments is studied. Four processes of relaxation of dipole polarization, γ-, β-, β_1-, and α-processes are identified by the method of dielectric spectroscopy. Monte-Carlo conformational analysis and molecular dynamics of dimeric chain fragments of these polymers is performed and mobilities of specific chain fragments are estimated. Molecular mechanisms for the γ-, β-, and β_1-processes, occurring in the glassy state, are suggested on the basis of a comparison of the dielectric spectroscopy and molecular modeling data.

© 2012 Elsevier B.V. All rights reserved.

1. Introduction

At present, polymers functionalized with organic moieties providing specific applications are of great interest. The introduction of nonlinear optical chromophores into macromolecules allows one to prepare materials exhibiting nonlinear optical (NLO) response to a laser irradiation [1–6]. Such materials are promising for the creation of operating elements for optoelectronics, holography, and communication devices.

In particular cases, chromophore-containing polymers exhibit quadratic NLO characteristics – second harmonic generation (SHG) coefficient, d_{33}, and electrooptical coefficient, r_{33}, not only comparable to but even exceeding the corresponding values for typical inorganic NLO crystals such as $LiNbO_3$ [5–7]. Important advantages of NLO polymers as compared to the inorganic NLO materials are high NLO susceptibility, fast NLO response, low dielectric constants, low refraction index dispersions from dc to optical frequencies, virtually endless possibilities of structural modification, an easy processability, and the possibility to form thin films of a high optical quality.

Up to now, many polymers with quadratic NLO activity were synthesized, yet the problem of transformation of the molecular NLO response into the macroscopic NLO response of the material still remains an urgent one. As the quadratic NLO activity may be exhibited only in macroscopically non-centrosymmetric materials, a polar ordering of chromophore groups in a material should be created. This ordering is achieved as a result of the alignment of chromophores under an external static electric field, in particular, in the corona charge field, which is applied to the material heated to the temperature close to the glass transition temperature, T_g. The achieved macroscopic polarization is frozen by the subsequent cooling down to room temperature, the electric field being released only afterwards. Thus, the material acquires the properties of a polymer electret. A reorientation of chromophore groups in a chromophore-containing polymer under an external electric field is provided by its molecular mobility. The dielectric spectroscopy (DS) gives important information on the polymer structure, molecular mobility, and intermolecular interactions. Polar groups, being the constituents of macromolecules, serve as natural labels at the observation of various forms of molecular motions, allowing one to establish the regions of maxima at the frequency and temperature curves of dielectric loss tangent, $tg\Delta$, and dielectric loss factor, ε''. These regions are related to the processes of relaxation of the dipole polarization of polar kinetic units, in particular, chromophore groups and their fragments [8,9].

An additional tool to study the orientational dynamics of chromophores in a polymer matrix is provided by molecular modeling (MM), which may be helpful for predicting structures with the optimal orientation order of chromophore groups and thus promising NLO response properties [10–16]. The modeling gives insight into physical mechanisms of chromophores orientation and relaxation during the process of electret formation, which is essential for the development of NLO polymer materials combining a high nonlinearity with a good thermal stability. Computer simulations, allowing a detailed examination of molecular conformations inaccessible by experimental means, provide a useful link between theory and experiment, ensuring the interpretation of DS data on the

* Corresponding author.
E-mail address: n_nikonorova2004@mail.ru (N.A. Nikonorova).

0009-2614/$ - see front matter © 2012 Elsevier B.V. All rights reserved.
http://dx.doi.org/10.1016/j.cplett.2012.09.053

motion of chromophore groups. Several research teams have studied the electric field poling of NLO polymers [10–16]. Monte-Carlo simulations of the poling field effect on the orientation of NLO chromophores in inert PMMA and amorphous polycarbonate matrices with the account of dipole–dipole electrostatic interactions of the chromophore groups were performed [10,11]. The poling process dynamics and the poling field effect on the SHG relaxation for various polymer systems were studied by a fully atomistic MM of poled guest–host NLO polymer systems at different densities [12]. Static conformational properties, radial distribution functions and energetics in poled and unpoled systems of PMMA doped with a NLO chromophore, *N*,*N*-dimethyl-*p*-nitroaniline (DPNA), were examined. The poling process in side-chain polyimides was examined by molecular dynamics (MD) simulations [17]. The stability of the poling-induced alignment in linear epoxy polymers with tolane chromophores was studied by SHG and dielectric spectroscopy [18]. Dependences of the epoxy backbone conformation and the molecular mobility on the structure and electric properties of incorporated chromophores were studied by atomistic simulations and semi-empirical quantum-chemical calculations [19].

In the present Letter, the dielectric behavior of two epoxy-based oligomers containing hydroxyl and methacryloyl groups – CFAO and CFMAO, respectively, with covalently attached 4-amino-4′-nitroazobenzene NLO chromophore fragments are studied (Figure 1).

The purpose of the Letter is a molecular identification of the observed dipole polarization relaxation processes in CFAO and CFMAO, and a comparative study of their kinetic characteristics of molecular mobility.

2. Experimental

CFAO was synthesized via a post-functionalization of an oligoepoxyamine precursor by azocoupling of its aromatic units with stable diazonium salts [20]. According to the data of elemental analysis and ^{1}H NMR spectroscopy, the attained functionalization degree of CFAO aniline groups was 96% [20]. Therefore, azochromophores are not exposed to rather severe polymerization conditions employed for the synthesis of the precursor. Moreover, this synthetic procedure makes it possible to obtain oligomers with high molecular weight (M_w = 24200, M_w/M_n = 2.12) and high content of azochromophores (41.6 mol%) with a good yield.

To fix a poling-induced non-centrosymmetric ordered arrangement of chromophores, a cross-linking of oligomer chains in their poled state is often utilized. In particular, CFAO may be cured into polymer networks by diisocyanates, but this approach faces problems caused by a rather high sensitivity of diisocyanates to atmospheric moisture and by difficulties of a synchronization of the cross-linking and poling processes. In order to avoid these problems, we prepared self-curing CFMAO oligomers (M_w = 10300, M_w/M_n = 1.76) with methacryloyl groups instead of hydroxyl ones, treating CFAO with methacryloyl chloride in the presence of triethylamine and *N*,*N*-dimethylaminopyridine [21].

The glass transition temperatures of CFAO and CFMAO were measured on a 'Metler Toledo DSC-822' differential scanning calorimeter with the heating/cooling rate ten degree/min. Samples were weighted on high-precision 'Metler Toledo AX-105' balances with the precision of 10^{-5} g. According to the data of differential scanning calorimetry (DSC), T_g values for CFAO and CFMAO are 130 and 110 °C [21], respectively.

Dielectric spectra were recorded on a 'Novocontrol' broadband dielectric spectrometer with an ALPHA-ANB high-resolution automatic frequency-analyzer. The measurements were performed under nitrogen in the frequency range 10^{-2}–10^7 Hz for temperatures from −155 to +200 °C. Samples were pressed between brass electrodes (the diameter of the upper electrode is 10–20 mm) at a temperature exceeding T_g by 30–50 °C. The sample thickness is fixed by a 50 μm silica fiber between the electrodes.

MM of the studied oligomers was performed in the framework of a Monte-Carlo conformational search of dimeric chain fragments giving the set of unique conformations within the 5 kcal/mol window relative to the global minimum [22]. Three characteristic conformers (A, B, and C) differing by the mutual arrangement of chromophore moieties were selected. The distribution of the torsion angles values for these conformers is studied by molecular dynamics, the simulation being performed in a dielectric medium with the dielectric permittivity ε' = 4.8. The following values of the simulation parameters are used: time step 1.5 fs; equilibration time 1 ps; simulation time 1 ns. The GB/SA continuum model [23] was used for the account of the environment effect. In the figures below, only the distributions of angles for one conformer are presented. Earlier, we showed that the oligomer with a short chain length may be considered as a good model for studying the conformational properties [19]. All calculations were performed with the use of MMFF94s force field [24] in the framework of Macromodel program package [25].

For measurements of nonlinear optical characteristics polymer films were spin-cast from CFAO and CFMAO solutions in cyclohexanone [21]. In order to induce a non-centrosymmetric arrangement of chromophore groups, the films were poled in the corona field under 6.5–7 kV voltage, the distance from a tungsten needle electrode to the surface of the film being 1 cm. The orientational order parameter of chromophore groups was controlled by

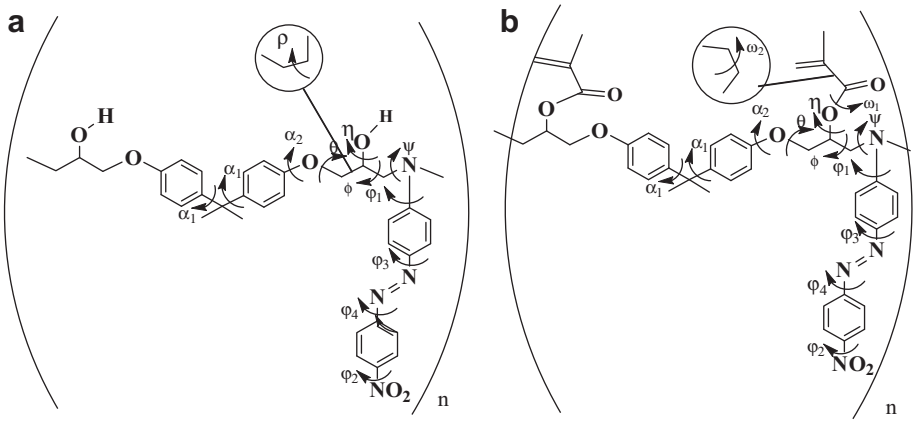

Figure 1. Structure of the monomeric unit of the oligomers under study: CFAO (a) and CFMAO (b).

UV-spectroscopy on the basis of the change in the chromophore absorbance values before (A_0) and after (A) poling: $\eta = 1-A/A_0$.

Polymer NLO properties were studied by Second Harmonic Generation (SHG) technique on an automated unit with α-quartz (x-cut) plate as a standard; the fundamental beam was provided by pulse Nd^{3+}:YAG laser ($\lambda = 1064$ nm, pulse duration 15 ns, power density at the sample 10 kW/cm^2) [21]. SHG coefficients, d_{33}, were obtained from the best fit of the calculated angular dependences of SHG intensities to the experimental data.

3. Results and discussion

3.1. General features of the dielectric behavior of CFAO and CFMAO

The dielectric behavior of CFAO and CFMAO in the studied ranges of temperatures and frequencies are qualitatively similar. In Figure 2, the temperature dependences of $tg\Delta = \varphi(T)$ at various frequencies are presented for an example of CFAO. In the range from −155 to +200 °C, four relaxation processes are observed denoted as γ-, β-, β_1- and α-processes, in the order of increasing temperature. The γ-, β-, β_1-processes are observed in the glassy state, while the α-process is realized in the rubber state.

The most important characteristic of each relaxation process is the most probable relaxation time, τ_{max}, determined, according to [26] as

$$\tau_{max} = \tau_{HN}\left[\frac{\sin\left(\frac{\pi\alpha_{HN}\beta_{HN}}{2(\beta_{HN}+1)}\right)}{\sin\left(\frac{\pi\alpha_{HN}}{2(\beta_{HN}+1)}\right)}\right]^{1/\alpha_{HN}} \quad (1)$$

The parameters τ_{HN}, α_{HN}, and β_{HN}, in turn, are estimated from frequency dependences of the complex permittivity, $\varepsilon^* = \varepsilon'(\omega) - i\varepsilon''(\omega)$, described by the empirical Havriliak–Negami equation [27] for one ($k = 1$) or a sum of two ($k = 2$) relaxation processes:

$$\varepsilon^*(\omega) - \varepsilon_\infty = \sum_{k=1}^{n} \mathrm{Im}\left[\frac{\Delta\varepsilon_k}{\{1 + (i\omega\tau_{HN_k})^{\alpha_k}\}^{\beta_k}}\right] \quad (2)$$

Here, $\omega = 2\pi f$, $\Delta\varepsilon = \varepsilon_0 - \varepsilon_\infty$ is the increment of dielectric permittivity ($\varepsilon_0 = \varepsilon'$ at $\omega \to 0$, $\varepsilon_\infty = \varepsilon'$ at $\omega \to \infty$), τ_{HN} is Havriliak–Negami relaxation time, α_{HN} and β_{HN} are fitting parameters, corresponding to width and asymmetry of the relaxation times distribution, respectively.

In the rubber state, the dc conductivity contribution into $\varepsilon^*(\omega)$, appearing at low frequencies, was accounted as $\frac{\sigma_{dc}a}{\varepsilon_v\omega^s}$ [28] where σ_{dc} is the specific dc conductivity, a is a constant having dimension $[a]=[\mathrm{Hz}]^{s-1}$, $s < 1$, ε_v is the permittivity of vacuum.

Frequency dependences of the dielectric losses factor, $\varepsilon'' = \varphi(f)$, for CFAO in the range of β_1- and α-processes and for CFMAO in the range of γ- and β-processes are presented in Figure 3a and b, respectively. They are satisfactorily described by Eq. (2). As an example, in Figure 4a, the dependence $\varepsilon'' = \varphi(f)$ is presented at 120 °C as a sum of β_1- and α-processes for CFAO and in Figure 4b, at −100 °C as a sum of γ- and β-processes for CFMAO.

Dipole polarization relaxation times for γ-, β-, β_1-, and α-processes, determined according to Eq. (1), are presented for CFMAO and CFAO polymers in Figure 5.

In the region of γ-, β-, and β_1-processes, the dependences $-\log\tau_{max} = \varphi(1/T)$ are linear (Figure 5, curves 1, 1′, 2, 2′, and 3, 3′, respectively) and are described by the Arrhenius equation, assuming the single relaxation process:

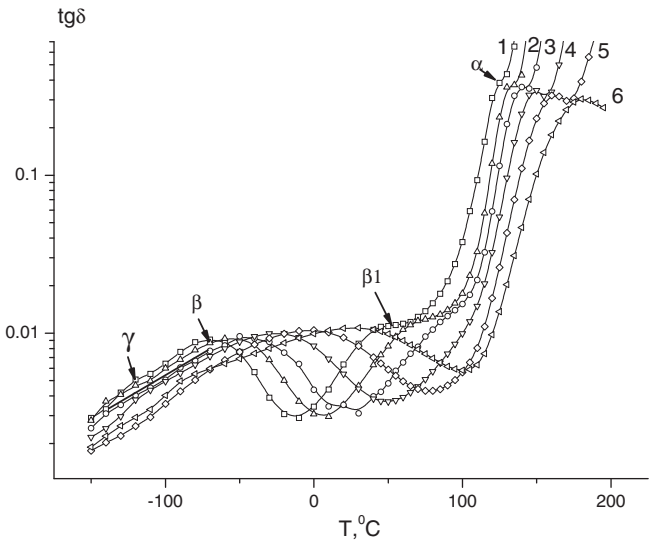

Figure 2. Temperature dependence of dielectric loss at 0.0005 (1), 0.005 (2), 0.05 (3), 0.5 (4), 5 (5), and 50 kHz (6) for CFAO.

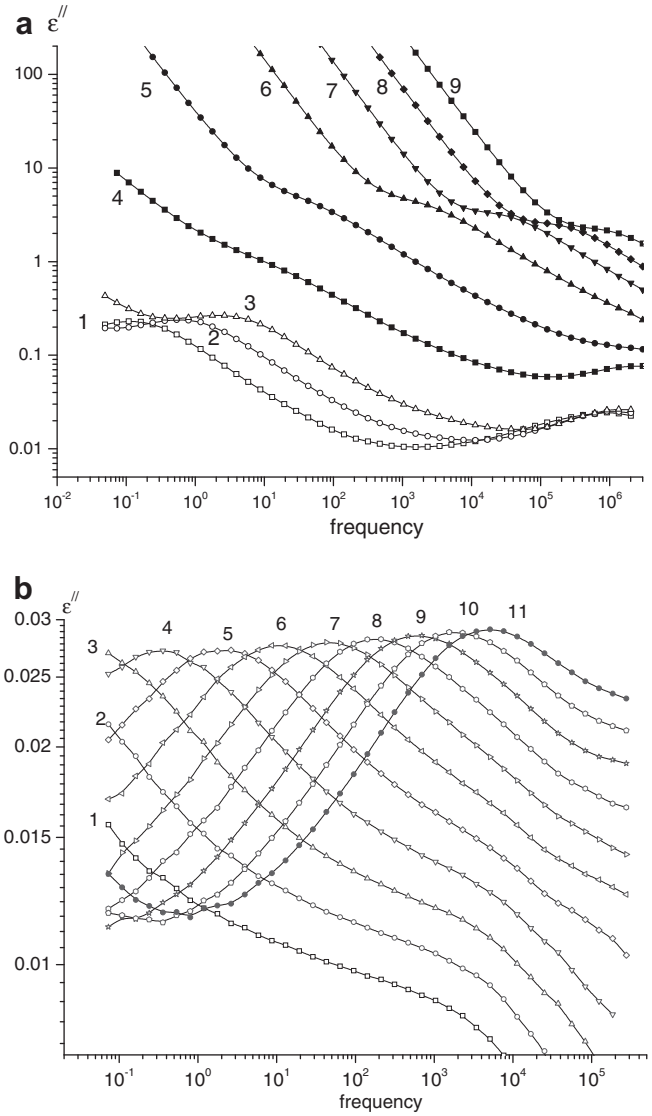

Figure 3. Frequency dependencies of ε'' in the range of β_1–и α-processes for CFAO at 60 (1), 80 (2), 100 (3), 120 (4), 140 (5), 160 (6), 180 (7), 200 (8), and 220 °C (9) (a) and in the range of γ- and β-processes for CFMAO at −130 (1), −120 (2), −110 (3), −100 (4), −90 (5), −80 (6), −70 (7), −60 (8), −50 (9), −40 (10), and −30 °C (11) (b).

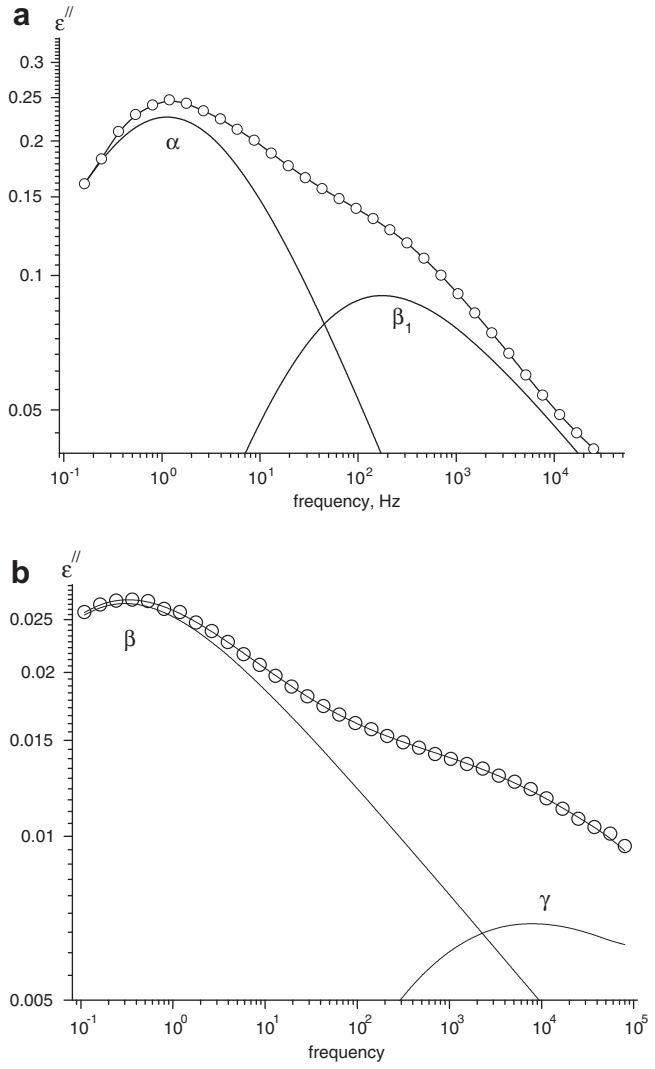

Figure 4. Frequency dependences of ε'' for CFAO at 120 °C (subtraction of dc conductivity) (a) and for CFMAO at −100 °C, (b) described according to the HN equation by the sum of β_1- and α- and γ- and β-processes, respectively. HN parameters for β_1-process: $\Delta\varepsilon = 0.28$, $\alpha_{HN} = 0.62$, $\beta_{HN} = 0.44$, $\tau_{max} = 9.04 \cdot 10^{-4}$ s, for α-process: $\Delta\varepsilon = 0.95$, $\alpha_{HN} = 0.57$, $\beta_{HN} = 0.98$, $\tau_{max} = 0.14$ s, for γ-process: $\Delta\varepsilon = 0.068$, $\alpha_{HN} = 0.45$, $\beta_{HN} = 0.23$, $\tau_{max} = 1.85 \cdot 10^{-5}$ s, and for β-process: $\Delta\varepsilon = 0.18$, $\alpha_{HN} = 0.56$, $\beta_{HN} = 0.34$, $\tau_{max} = 0.52$ s.

$$\tau(T)_{max} = \tau_0 \exp\left(\frac{E_a}{RT}\right) \quad (3)$$

$\tau_0 = \tau_{max}$ at $T \to \infty$, E_a is the activation energy, R is the absolute gas constant. Values of $-\log \tau_0$ and E_a for γ-, β- and β_1-processes are presented in Table 1.

A linear dependence $-\log \tau_{max} = \varphi(1/T)$ is characteristic of local forms of mobility. The reorientation of small kinetic units (polar groups, atoms) is virtually non-correlated with the neighboring chains, the motion kinetics being controlled by intramolecular interactions. For local forms of mobility, τ_0 and E_a are about 10^{-11}–10^{-13} s and 4–12 kcal/mol, respectively.

In the α-process region, the relaxation time temperature dependences for CFMAO and CFAO are nonlinear (Figure 5, curves 4, 4′, respectively) and may be described by the Vogel–Fulcher–Tammann–Hesse equation [29]:

$$\tau_{max} = \tau_0 \exp\left(\frac{B}{T - T_0}\right) \quad (4)$$

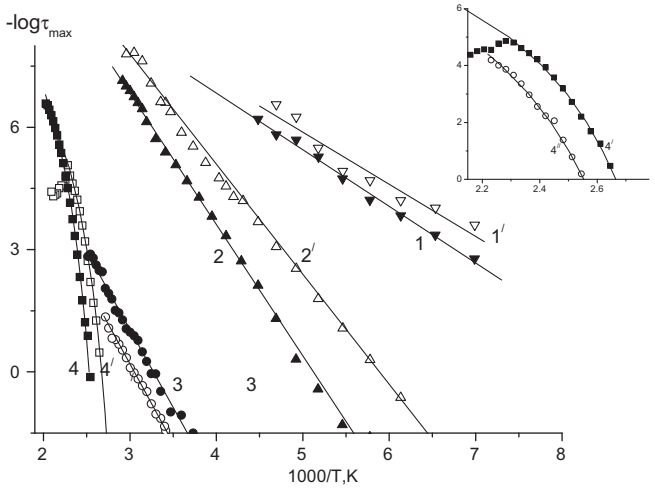

Figure 5. Dependences of $-\log \tau_{max}$ on reciprocal temperature for CFAO (1–4) and CFMAO (1′–4′) in the range of γ- (1,1′), β- (2,2′), β_1- (3,3′), and α- (4,4′) processes. The data for CFMAO sample before (curve 4′) and after its heat treatment above 160 °C (curve 4′′) are shown in the inset.

where τ_0, B and T_0 are temperature-independent parameters. T_0 is the so-called Vogel temperature, being usually several tens of degrees lower than T_g. The parameter B is a measure of nonlinearity of the dependence $-\log \tau_{max} = \varphi(1/T)$, the smaller is the B value, the higher is a cooperativity of the process under study. The values of the parameters of Eq. (4) for CFAO and CFMAO are presented in Table 2.

Nonlinearity of the $-\log \tau_{max} = \varphi(1/T)$ dependence is characteristic of cooperative forms of molecular mobility, the corresponding parameters being determined to a considerable extent by intermolecular interactions. Cooperative forms of molecular motions are characterized by a broad set of relaxation times and are realized as joint motions of a large number of kinetic units.

Defining molecular mechanisms of relaxation γ-, β-, β_1-, and α-processes in CFAO and CFMAO oligomers, one should take into account motions of their polar groups, including chromophore end nitro-groups (dipole moment $\mu = 4.01$ D) and polar groups in the main chain such as tertiary amino, ether, hydroxyl, and ester groups with $\mu = 1.3$, 1.4, 1.5, and 1.8 D [30], respectively (trans-azo group has zero dipole moment). Dielectric properties of CFAO and CFMAO are due to the molecular mobility related to internal rotations (torsions) of polar kinetic units around the chemical bonds denoted by arrows in Figure 1. These rotations are dielectrically active as they change the dipole moment projection on the electric field direction, thus being an origin of dielectric absorption.

In the present Letter, molecular mechanisms of the γ-, β-, β_1-, and α-processes in CFAO and CFMAO oligomers are analyzed in the framework of the widely recognized interpretation of dielectric processes in polymers with similar architectures, such as comb-like copolymers with functional (mesogenic, chromophore) side groups [31–34] and main-chain aromatic polyesters [35–37]. It should be kept in mind that in the polymers under investigation, the backbone and chromophores motions are strongly coupled due to the fact that the amino groups of chromophores are incorporated into the backbone.

3.2. γ-Process

For polymers whose molecular architecture is similar to that for the systems studied in this Letter the region of the lowest-temperature (the fastest) γ-process is known to be caused by the mobility of polar end-groups. For CFMAO and CFAO temperature–frequency

Table 1
Parameters of Eq. (3) for the γ-, β-, and β_1-processes.

Sample	$-\log\tau_0$ (s) γ-process	E_a kcal/mol	$-\log\tau_0$ (s) β-process	E_a kcal/mol	$-\log\tau_0$ (s) β_1-process	E_a kcal/mol
CFAO	12.4	6.4	16.5	14.8	12.50	17.7
CFMAO	12.3	6.0	15.9	12.4	11.6	17.5

Table 2
$T_{g(DS)}$ and $T_{g(DSC)}$ values and parameters of Eq. (4) for the α-process.

Polymer	$-\log\tau_0$ (s)	B, K	T_0, K	$T^a_{g(DS)}$ (°C)	$T_{g(DSC)}$ (°C)
CFAO	10.9	1496	336	122	130
CFMAO	9.7	1279	318	102	110
Heated CFMAO	9.6	1541	322	119	–

[a] T_g is determined at $\log\tau_{max} = 0$.

coordinates of this process (Figure 5, curves 1 and 1′, respectively) are close to those for chromophore-containing comb-like copolymethacrylates with polar end groups [31–34]. In the case of CFAO and CFMAO, it seems to be determined by reorientations of polar end NO_2 groups.

The parameters of Arrhenius equation for the γ-process in CFAO and CFMAO are close to each other and are characteristic of local forms of the Debye-type molecular mobility with a single relaxation time (Table 1). As expected, the structure of the backbone almost does not affect the mobility of the end groups.

MM reveals several maxima on the distribution curves for the torsion angle φ_2 (Figure 6a) and for angles η describing the rotation of hydroxyl hydrogen (dielectrically inactive rotation) in CFAO (Figure 6b) and methacryloyl groups in CFMAO (Figure 6c). The range of accessible η angles for CFMAO is essentially narrower than that in the case of CFAO due to presence of bulky methacryloyl groups (Figure 6d). Moreover, ω_2 torsions within the methacryloyl groups in CFMAO are just initiated at the temperatures of the γ-process (Figure 6c).

Thus, both DS and MM studies confirm that γ-processes arise in CFAO and CFMAO due to rotations of end NO_2 groups in both polymers and methacryloyl groups in CFMAO.

3.3. β-Process

The γ-process is followed by the β-process on the temperature scale. Locations of the β-processes on the $-\log\tau_{max} = \varphi(1/T)$ plot (Figure 5, curves 2 and 2′) for CFAO and CFMAO are close to that for comb-like polymers [31–34] and main-chain aromatic polyesters [35–37]. It has been shown that the β-process in comb-like polymers is represented by rotations of functional side groups about their long axes. For main-chain aromatic polyesters, the occurrence of the β-process was related to hindered reorientations of small kinetic units of the backbone. Therefore, it may be

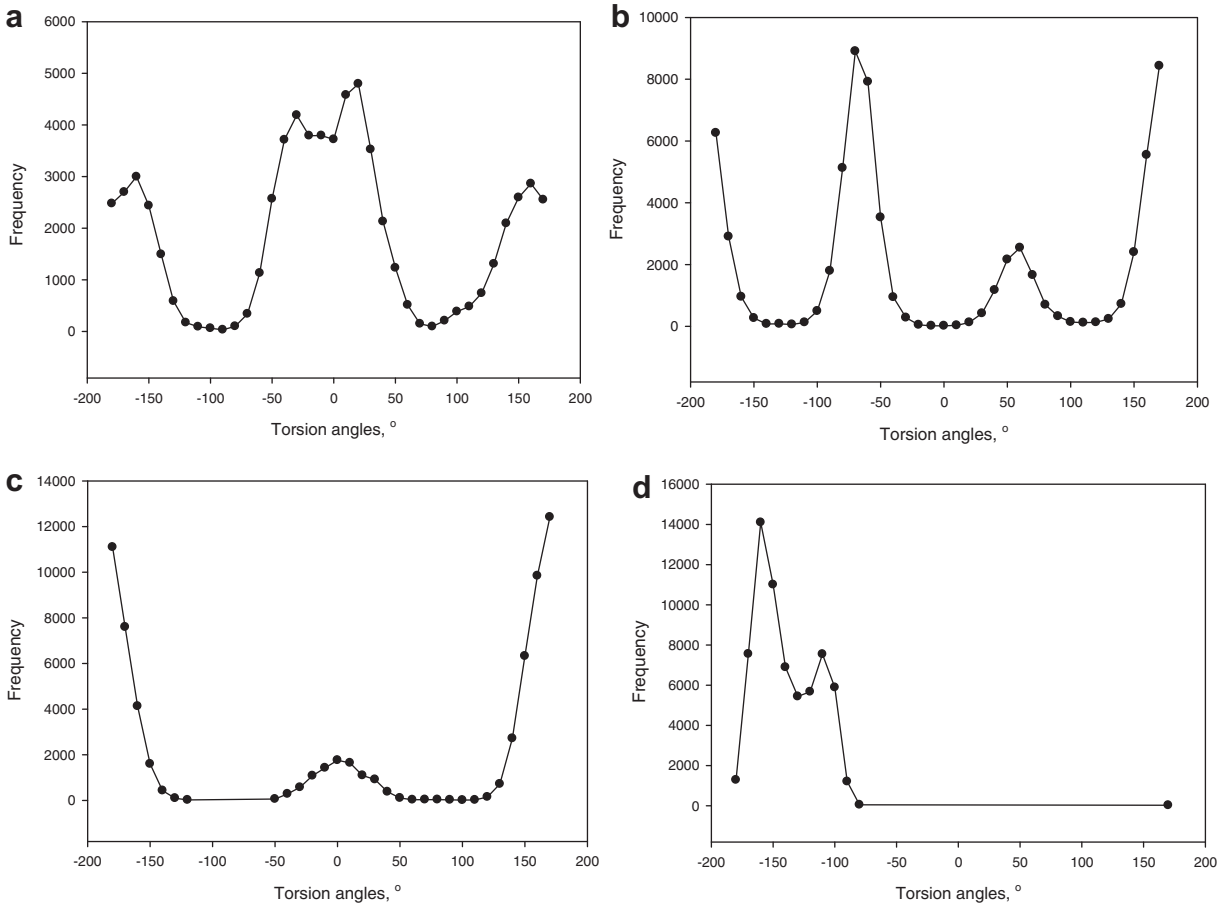

Figure 6. Distributions of φ_2 (a) and η (b) angle values for CFAO dimer and ω_2 (c) and η (d) for CFMAO dimer of at $T = -120$ °C.

assumed that the molecular origin of the β-process in CFAO and CFMAO is a result of a superposition of the local mobility of chromophore groups (φ_1 torsion) and local reorientations of polar groups in the backbone.

Parameters of Arrhenius equation for the β-process are higher than those for the local mobility modes (Table 1). This means that molecular mobility is determined not only by the nearest environment but by the intermolecular interactions as well. A comparison of curves 2 and $2^{/}$ shows that the β-process relaxation time for CFAO is one-two orders of magnitude higher than that for CFMAO, where bulky methacryloyl groups make the polymer structure less dense and reduce intermolecular interactions.

MM for CFAO at –70 °C (close to the β-process) show that reorientations in bis-phenol fragments described by α_1 angles (Figure 1) contribute to the β-process (Figure 7a). As to CFMAO, the mobility in the bis-phenol fragment seems to occur at 50 °C, temperatures being higher than that of the β-process (Figure 7b). It can rather be attributed to the following β_1-process.

In contrast to DS data, MM calculations do not detect the rotations of the azochromophore groups described by the φ_1 angle. However, MM data show that the mobility inside of azo-fragments described by φ_3 and φ_4 angles is found.

3.4. β_1-Process

The β_1-process precedes the α-process on the temperature scale and is observed in the glassy state. The temperature dependences of relaxation times for CFAO and CFMAO (Figure 5, curves 3 and $3^{/}$, respectively) are close to those observed in linear polyesters [35–37]. It is assumed that the β_1-process in linear polyesters is related to reorientations (in the glassy state) of short backbone fragments, involving polar groups.

Arrhenius equation parameters for the β_1-process exceed considerably those for the local modes of molecular mobility, demonstrating that the β_1-process is affected by intermolecular interactions. In the range of the β_1-process, the $-\log\tau_{max} = \varphi(1/T)$ dependence for CFAO lies at lower temperatures than that for CFMAO (Figure 5, curves 3 and $3^{/}$, respectively). This means that molecular mobility for the β_1-process for CFAO is higher than that for CFMAO.

MM makes it possible to identify certain backbone fragments contributing to the β_1-process. According to the data of MM, one can suppose that for CFAO (Figure 8b) and CFMAO (Figure 8c) these backbone fragments are bis-phenol moieties with adjacent ether groups (motions described by the α_2 angles). Moreover, for CFAO, a contribution to the β_1-process is provided by reorientations of OCCO main-chain fragments related to the ρ angle (Figure 8a). In the case of CFMAO, the molecular motions described by the ρ angle are exhibited in the intermediate temperature range between β_1- and α- processes, making their exact assignment difficult.

3.5. α-Process

For CFAO and CFMAO, the highest-temperature α-process is related to the main chain segmental motion and reflects a transition from the glassy to the rubbery state. The glass transition temperatures were determined from the DS data by the extrapolation of curves 4 and $4^{/}$ in Figure 5, respectively, described by Eq. (4), to $\log\tau_{max} = 0$. T_g estimated from the DS data are found to be close to T_g values determined by the DSC technique (Table 2). The lower T_g value for CFMAO as compared to that for CFAO is caused by a decreased molecular packing density due to the presence of bulky methacryloyl groups (plasticization effect).

The presence of reactive methacryloyl groups in CFMAO results in the polymer cross-linking upon heating above 110 °C [38]. This ability of CFMAO to form cross-linked systems is important for the thermal stability of its NLO activity. The process of cross-linking can be seen in the dependence $-\log\tau max = \varphi(1/T)$ for CFMAO as a deviation of relaxation time values from curve $4^{/}$ (Figure 5). After this heat treatment, the dependence $-\log\tau_{max} = \varphi(1/T)$ for CFMAO (curve $4^{/}$) is shifted to higher temperatures (curve $4^{//}$, inset in Figure 5). It means that the segmental molecular mobility of the main chain is reduced and the T_g value increases (Table 2).

The performed MM of short oligomeric chain fragments does not allow to interpret the experimental DS data on the α-process, because this is a large-scale cooperative process determined mainly by intermolecular interactions. An attempt to describe it in terms of local mobility of chain fragments would be not appropriate.

3.6. NLO characteristics

Earlier, we observed that the poling efficiency is affected essentially by the poling protocol as well as the procedure of film preparation [38]. In accordance with the data presented here, more efficient poling of CFAO films and resulting values of d_{33}

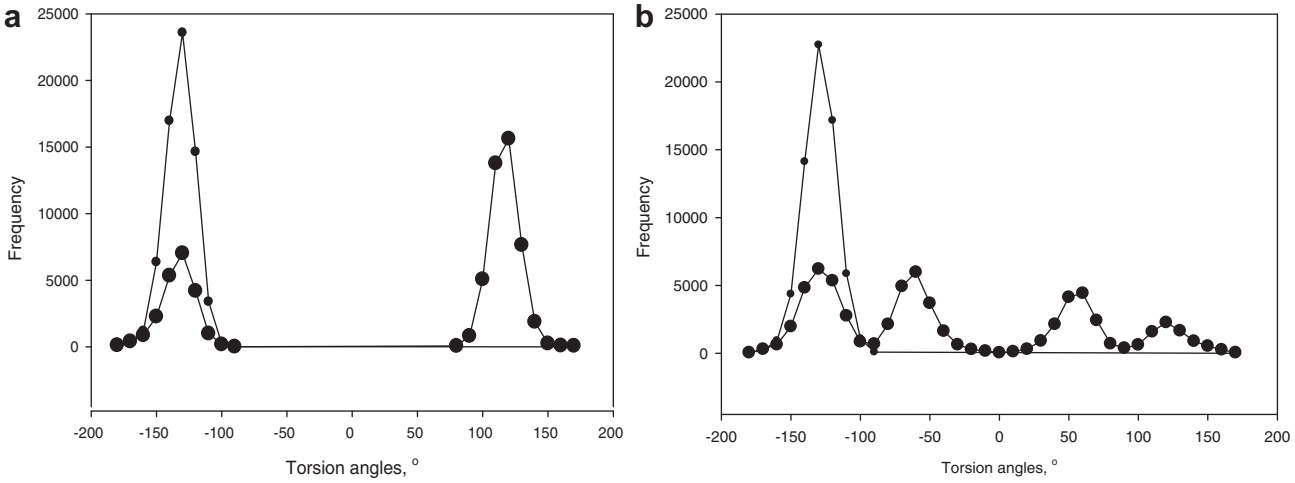

Figure 7. Distributions of α_1 angle values for CFAO dimer at T = –120 and –70 °C (a) and for CFMAO dimer at T = –70 and 50 °C (b); small circles – for lower temperature, large circles – for higher temperature.

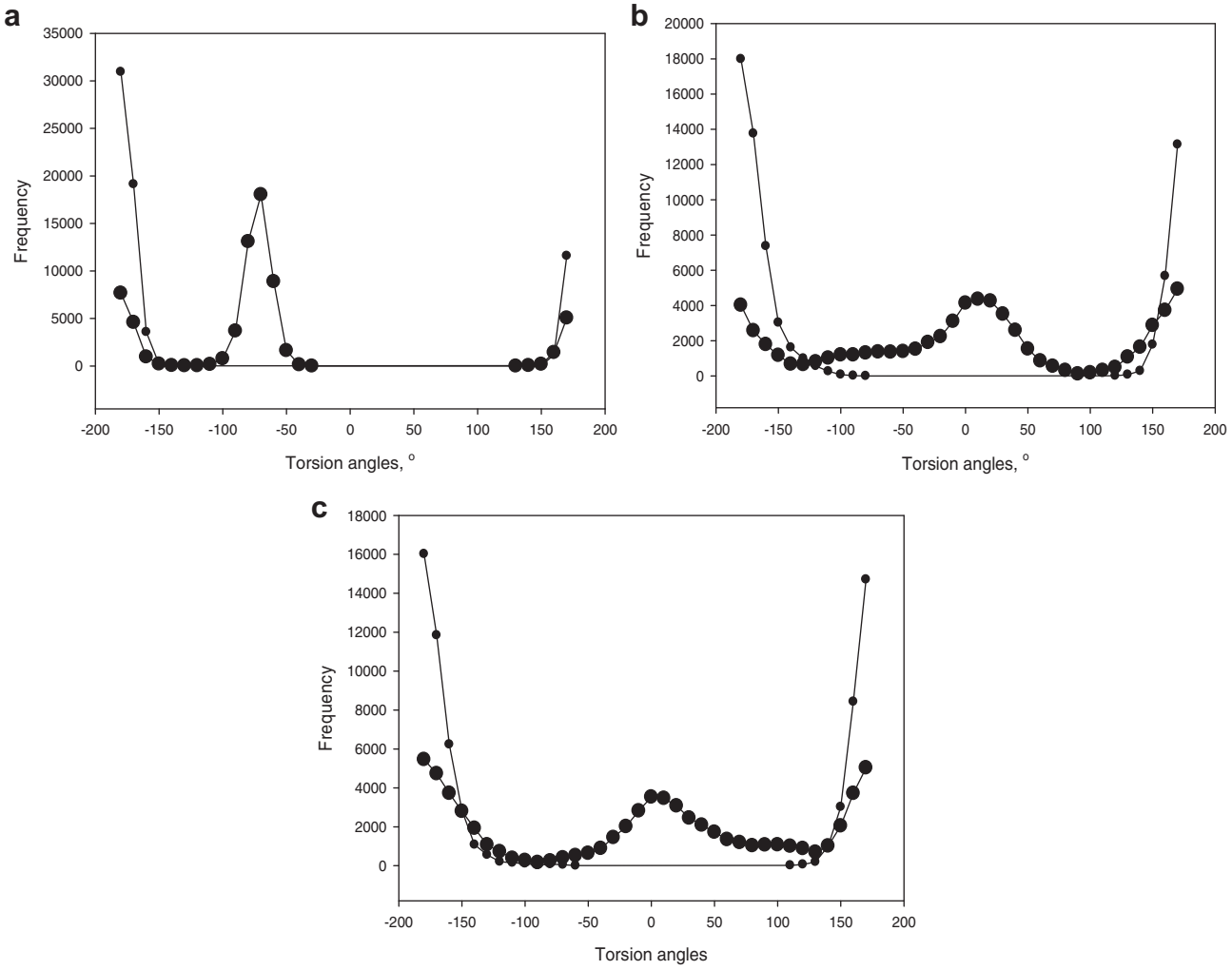

Figure 8. Distributions of ρ (a) and α_2 (b) angle values for CFAO dimer and α_2 (c) for CFMAO dimer at T = –70 and 50 °C; small circles – for lower temperature, large circles – for higher temperature.

Table 3
Film thickness (h), poling temperature (T_p), order parameter (η), and SHG coefficients (d_{33}) of the studied polymer films.

Sample number	Polymer	h, nm	T_g (°C)	T_p (°C)	η	d_{33} (pm/V)
1	CFAO	390	130	110	0.16	28.9
2		260		120	0.28	62.0
3	CFMAO	200	110	110[a]	0.14	21.3
4		260		110[b]	0.20	35.0

[a] The corona-field was switched on at 110 °C.
[b] The corona-field was switched on at 90 °C.

coefficients are obtained when higher poling temperatures are used (see Table 3, samples 1 and 2). One may expect even higher values of d_{33} when T_p is close to 130 °C, i.e. equal to T_g. As for CFMAO films, T_p was chosen equal to T_g (110 °C), however the poling procedure was somewhat different: in the case of sample 3 the field was switched on just when T_p was reached, whereas when the sample 4 was poled, the field was switched on at lower temperature (90 °C) and the further increase of temperature up to T_p = 110 °C was carried out. The data of Table 3 demonstrates that the second procedure seems to be more efficient for CFMAO (sample 4), as according to the study of cross-linking kinetics based on the IR-spectral data, the cross-linking process already starts at 110 °C. Thus, using the second procedure of poling (sample 4), we obtained higher values of d_{33} coefficients.

4. Conclusions

To conclude, four relaxation processes were observed in CFAO and CFMAO polymers: the γ-, β-, and β_1- processes - in the glassy state and the α-process – in the rubbery state. Molecular mechanisms of these processes were proposed on the basis of the DS and MM (for the glassy state processes) data.

According to the DS and MM data, the γ-process reflects the mobility of end nitro-groups in chromophore fragments for both CFAO and CFMAO and methacryloyl groups (for CFMAO). The β-process for CFAO and CFMAO is related to rotations of chromophores about their long axes and to local motions inside of chromophore. For CFAO, phenyl rings in bis-phenol fragments contribute also into the β-process. For the β_1-process, specific main chain fragments responsible for its occurrence were defined as phenyl rings in bis-phenol moieties with adjacent ether groups for CFAO and CFMAO. Additionally, OCCO backbone moieties contribute to the β_1-process in the case of CFAO. Finally, the α-process corresponds to the segmental motion of polymer chains. In the case of CFMAO, a decrease in the mobility due to cross-linking, resulting in a growth of T_g, becomes noticeable in dielectric spectra upon heating above 160 °C.

Upon the replacement of methacryloyl groups for hydroxyl ones, molecular mobility increases for the α- and β-processes, decreases for the β_1-process, and remains almost unchanged for the γ-process.

As follows from the data presented in Figure 5 (curves 4 and 4′ for α-processes in CFAO and CFMAO, respectively) the relaxation time, τ_{max}, for CFMAO sample is about two orders of magnitude lower than that for CFAO sample. Thus, it may be concluded that, in general, CFMAO sample is characterized by higher molecular mobility than CFAO sample. However, in spite of this fact, higher second order nonlinear optical coefficients, d_{33}, were not obtained for CFMAO samples as the cross-linking process starts already at T_p, making the orientation of chromophore groups more difficult. Subsequent cross-linking of methacryloyl group in CFMAO sample makes it possible to fix the attained polar orientation of chromophore groups, thus enhancing the stability of NLO properties.

Thus, the performed research allows one to conclude that an efficient poling of CFAO should be carried out at the temperatures not lower than 130 °C, when the mobility of chromophore groups and segments of the main chain arises. Poling of CFMAO is complicated by cross-linking starting from ~110 °C. Therefore, a further optimization of the temperature regime of CFMAO poling is necessary in order to achieve its optimal second-order NLO properties. It should also be emphasized that the dielectric measurements were performed for non-poled samples. In the future, we plan to obtain dielectric spectra for the corona-poled films-electrets, in order to study the effect of poling on molecular mobilities of the presented chromophore-containing oligomers.

Acknowledgements

Financial support of Russian Foundation for Basic Research (Project no. 11-03-00959-a) and Polytechnic University of Valencia (Grant of 2011) is appreciated.

Appendix A. Supplementary data

Supplementary data associated with this article can be found, in the online version, at http://dx.doi.org/10.1016/j.cplett.2012.09.053.

References

[1] S.K. Yesodha, C.K.S. Pillai, N. Tsutsumi, Prog. Polym. Sci. 29 (2004) 45.
[2] Y.V. Pereverzev, O.V. Prezhdo, L.R. Dalton, Chem. Phys. Chem. 5 (2004) 1821.
[3] E. Riande, R. Diaz-Calleja, Electrical Properties of Polymers, Marcel Dekker Inc., New York-Basel, 2004.
[4] L.R. Dalton et al., Chem. Mater. 7 (1995) 1060.
[5] L.R. Dalton et al., Ind. Eng. Chem. Res. 38 (1999) 8.
[6] L.R. Dalton et al., J. Mater. Chem. 9 (1999) 1905.
[7] L.R. Dalton, P.A. Sullivan, D.H. Bale, Chem. Rev. 110 (2010) 25.
[8] G.P. Simon, Dielectric Spectroscopy of Polymers, in: J.P. Runt, J.J. Fitzgerald (Eds.), ACS Ser., Washington, 1997.
[9] N.G. McCrum, B.E. Read, G. Williams, Anelastic and Dielectric Effects in Polymeric Solids, Wiley, London, 1967.
[10] B.H. Robinson, L.R. Dalton, J. Phys. Chem. A104 (2000) 4785.
[11] R.D. Nielsen, H.L. Rommel, B.H. Robinson, J. Phys. Chem. B108 (2004) 8659.
[12] W.K. Kim, L.M. Hayden, J. Chem. Phys. 111 (1999) 5212.
[13] M. Makowska-Janusik, H. Reis, M.G. Papadopolous, I.G. Economou, N. Zakharopolous, J. Phys. Chem. B108 (2004) 588.
[14] A. Dhinojwala, G.K. Wong, J.M. Torkelson, J. Chem. Phys. 100 (1994) 6046.
[15] S.C. Brower, L.M. Hayden, J. Polym. Sci. B36 (1998) 1013.
[16] Z.Y. Cheng, S. Yilmaz, W. Wirges, S. Bauer-Gogonea, S. Bauer, J. Appl. Phys. 83 (1998) 7799.
[17] J.A. Young, B.L. Farmer, J.A. Hinkley, Polymer 40 (1999) 2787.
[18] D. Jungbauer, I. Teraoka, D.Y. Yoon, B. Reck, J.D. Swalen, R. Twieg, C.G. Wilson, J. Appl. Phys. 69 (1991) 8011.
[19] M.Y. Balakina, O.D. Fominykh, F. Rua, V. Branchadell, Int. J. Quantum Chem. 107 (2007) 2398.
[20] S.V. Shulyndin et al., Polym. Sci. 47 (2005) 808.
[21] T.A. Vakhonina et al., Mendeleev Commun. 21 (2011) 75.
[22] G. Chang, W.C. Guida, W.C. Still, J. Am. Chem. Soc. 111 (1989) 4379.
[23] D. Qiu, P.S. Shenkin, F.P. Hollinger, W.C. Still, J. Phys. Chem. 101 (1997) 3005.
[24] T.A.J. Halgren, Comput. Chem. 17 (1996) 490.
[25] MacroModel, version 9.8, Schrodinger, LLC., New York, 2010.
[26] R. Diaz-Calleja, Macromolecules 33 (2000) 8924.
[27] S. Havriliak, S. Negami, Polymer 8 (1967) 161.
[28] S.U. Vallerien, F. Kremer, C. Boffel, Liq. Cryst. 4 (1989) 79.
[29] H. Vogel, Phys. Z. 22 (1921) 645.
[30] P. Hedvig, Dielectric Spectroscopy of Polymers, Akademiai Kiado, Budapest, 1977.
[31] N.A. Nikonorova, N.N. Smirnov, V.V. Kudryavtsev, R. Diaz-Calleja, A.V. Yakimansky, J. Polym. Sci. 46 (2008) 1488.
[32] N.A. Nikonorova, R. Diaz-Calleja, A.V. Yakimansky, Polym. Int. 60 (2011) 1215.
[33] A. Schonhals, D. Wolf, J. Springer, Macromolecules 28 (1995) 6254.
[34] R. Zentel, G.R. Strobl, H. Ringsdorf, Macromolecules 18 (1985) 960.
[35] L.L. Burshtein, T.I. Borisova, S.V. Zhukov, N.A. Nikonorova, D.N. Asinovskaya, S.S. Skorokhodov, Polymer 40 (1999) 1881.
[36] T.I. Borisova, L.L. Burshtein, N.A. Nikonorova, T.P. Stepanova, S.S. Skorokhodov, Polym. Sci. 40 (1998) 30.
[37] L. Hardy, I. Stevenson, A. Fritz, G. Boiteux, G. Seytre, A. Schonhals, Polymer 44 (2003) 4311.
[38] T.A. Vakhonina, S.M. Sharipova, N.V. Ivanova, O.D. Fominykh, N.N. Smirnov, A.V. Yakimansky, M.Y. Balakina, Proc. SPIE 7993 (2011) 799307.